JOURNAL OF GEOPHYSICAL RESEARCH, VOL. 94, NO. D1, PAGES 1195–1210, JANUARY 20, 1989

Precipitation Fluctuations Over Global Land Areas Since the Late 1800's

HENRY F. DIAZ

Environmental Research Laboratories, NOAA, Boulder, Colorado

R. S. BRADLEY

Department of Geology and Geography, University of Massachusetts, Amherst

J. K. EISCHEID

Cooperative Institute for Research in Environmental Science, University of Colorado, Boulder

An analysis of southern hemisphere land precipitation records for the last 100 years indicates an increase in mean annual precipitation since the 1940's, with positive anomalies, compared to the 1921–1960 reference period, occurring during approximately the last 15 years in all seasons except southern summer (December–February). There is little or no temporal correlation with corresponding precipitation indices for the northern hemisphere (Bradley et al., 1987*a*). Furthermore, while trends in the northern hemisphere temperate regions were opposite those in the northern tropical areas, in the southern hemisphere both zones exhibit similar trends. The change toward higher precipitation in middle latitudes begins about 10 years earlier in the northern than in the southern hemisphere (in the 1940's versus the 1950's, respectively). For the northern hemisphere, the overall linear trend from 1890 to 1986 is not significantly different from zero. However, a decline is evident since the 1950's, primarily due to lower rainfall amounts south of about 30°N. Globally, the trend is toward higher values in annual and seasonal precipitation, except for the boreal summer season (June–August). Most of the observed increases, however, took place from about 1940 to the mid-1950's, after which time the record has displayed little overall trend, instead exhibiting decade-long fluctuations. The observations are only broadly consistent with zonally averaged profiles of precipitation changes derived from general circulation model (GCM) simulations of climate using doubled atmospheric CO_2 concentrations, although we note that there is considerable variability in precipitation response from one model to another. One possible discrepancy occurs in the northern hemisphere tropics, where most GCMs indicate relatively little change in precipitation in response to CO_2 doubling (Gutowski et al., 1988), whereas in the past couple of decades there has been a major decline in rainfall in this region. The overall increase in southern hemisphere precipitation is consistent with marine observations for the tropics and extratropical southern latitudes, which show an increase in sea surface temperature of about 0.3°C since the mid-1970's and an increase in surface wind speed of between 0.4 and 0.8 m/s since 1950. The potential increase in evaporation could have contributed to the observed rainfall trends. We note, however, that precipitation in tropical land areas is strongly influenced by the phases of the El Niño/Southern Oscillation (ENSO), being generally lower during warm events and higher during the opposite cold phase. The effects of the strong ENSO warm events of 1982–1983 and around 1940 are clearly evident in the global record, as are precipitation peaks during cold years, such as 1974–1975 and 1954–1956.

1. INTRODUCTION

In a recent study, *Bradley et al.* [1987*a*] analyzed the precipitation record for the northern hemisphere (NH) land areas since the middle of the nineteenth Century. One of the interesting findings of that study was the presence of opposing precipitation trends between subtropical (5°–35°N) and midlatitude (35°–70°N) regions over approximately the past 40 years. For the NH as a whole the record exhibits considerable interdecadal variability, but relatively little trend. Some seasonal differences were noted as well, with northern summer and autumn showing declining precipitation over the past several decades, whereas winter and spring generally displayed greater totals.

In this paper we extend the analysis to the southern hemisphere (SH) land areas and combine both sets of data to produce land precipitation indices for the tropics, subtropics, and extratropical latitudes, as well as a "global-average" continental index. The NH record has also been updated through 1986, and 58 additional stations have been added (about 4% of the previous total). Obviously, since the oceanic areas are very poorly represented in these indices (see Figure 1), we can not ascertain whether there have been long-term shifts from one region to the other. A satellite-derived index of tropical convection, however, is available from 1971 to the present [*Garcia*, 1985], and an analysis of that data set will be the subject of a separate study.

Our objectives were (1) to delineate the long-term temporal and spatial characteristics of precipitation variation in the southern hemisphere land areas from the available set of long-period station records; (2) to compare these results with those obtained in the earlier northern hemisphere study and to assess the degree of similarity of spatial changes during recent decades in comparison with general circulation model (GCM) experiments using doubled CO_2 concentrations; and (3) to examine some plausible mechanism that may have contributed to the observed changes.

Paper number 88JD03785.
0148-0227/89/88JD-03785$05.00

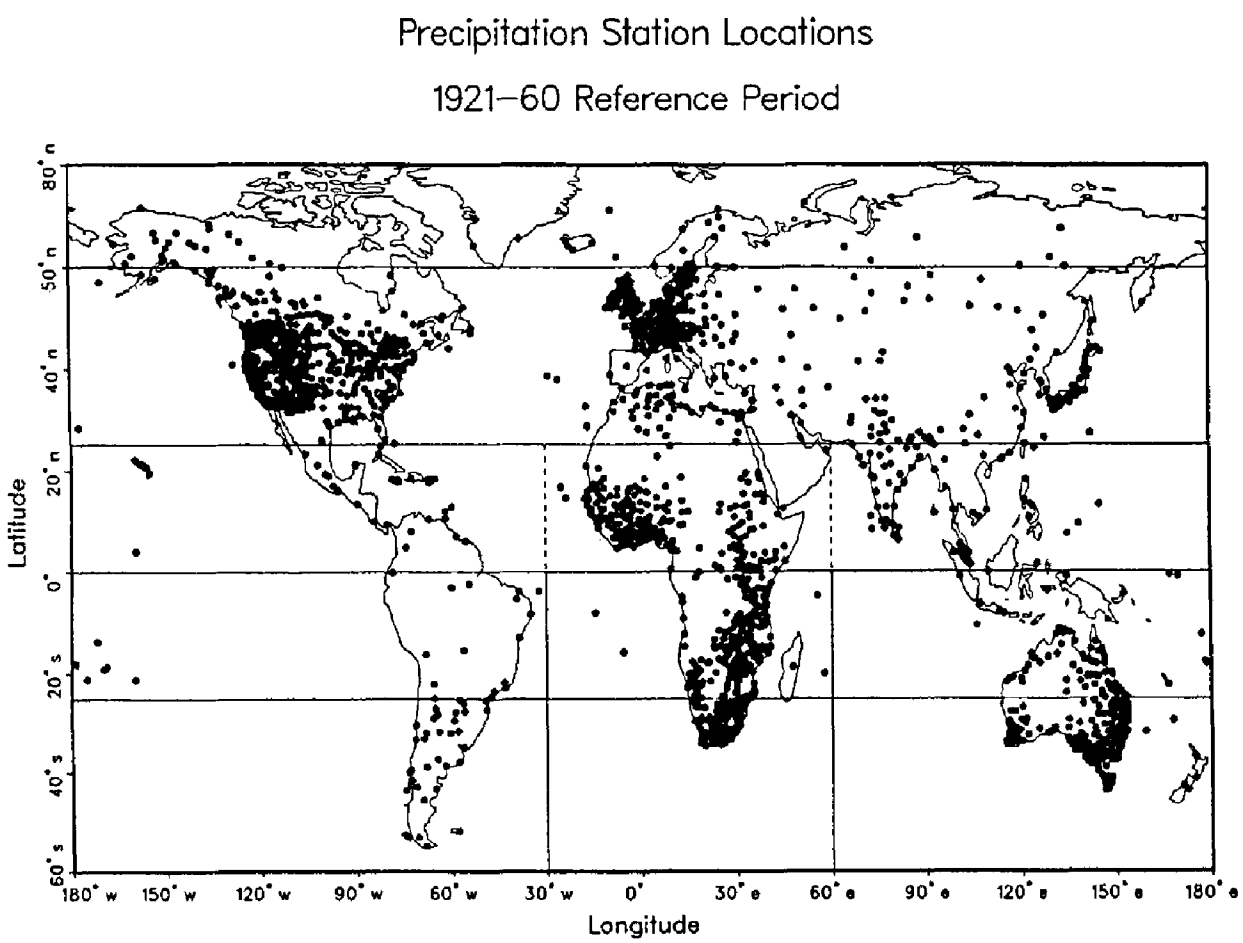

Fig. 1. Map showing location of stations and regions used in this study. Stations were selected on the basis of their having at least 35 years of data within the interval 1921–1960.

2. DATA AND METHODS

The data represent an extension of the set of monthly station records used by *Bradley et al.* [1987*a*]. Figure 1 shows the full spatial distribution of stations throughout the globe. We wished to account for the great spatial variability in precipitation amounts and the fact that precipitation frequency distributions are generally nonnormally distributed. The usual standardization procedures are thus somewhat meaningless when averaging over space. As in the work by *Bradley et al.* [1987*a*], the following procedure was used. Previous work has shown that monthly and seasonal rainfall probabilities can be estimated with good precision by the gamma distribution [*Strommen and Horsfield*, 1969; *Ropelewski and Jalickee*, 1984]. The gamma distribution is a two-parameter frequency distribution given by

$$f(x) = \frac{1}{\beta^{\gamma}\Gamma(\gamma)} x^{\gamma-1} e^{(-x/\beta)} \qquad \beta > 0 \qquad \gamma > 0 \qquad (1)$$

where x is the random variable (the precipitation amount), γ and β are the appropriate shape and scale parameters, and $\Gamma(\gamma)$ is the ordinary gamma function of γ. The technique used to calculate γ and β is that of *Thom* [1958]. A gamma function was fitted to each station series of seasonal and annual precipitation totals, using the reference period 1921–1960 (identical to that used for the northern hemisphere analysis) to compute the necessary parameters. The amounts were thus converted to equivalent probability values or percentile points of the gamma distribution (a number between 0 and 1). Hence a value of, say, 0.35 for a given year or season means that the precipitation amount for that period falls in the lowest 35% of the gamma distribution, given the estimated shape and scale parameters derived from the 40-year reference period.

The percentile values were objectively interpolated onto a uniform grid, with a spacing of approximately 400 km (see *Bradley et al.* [1987*a*], Figure 1*b*, for an example of the grid point network), using a space-filtering technique described by *Maddox* [1980]. These gridded values were then aggregated and averaged to form the regional indices. Hence variations of the time series toward higher or lower percentile values indicate a shift toward higher or lower levels in the cumulative precipitation distribution functions of the stations that make up that particular index. A total of 656 southern hemisphere stations were used. About half of these stations were supplied by P. D. Jones of the Climatic Research Unit, University of East Anglia [cf. *Jones et al.*, 1986*c*], and the other half were extracted from the World Monthly Surface Station Climatology data set of the National Center for Atmospheric Research (NCAR), Boulder, Colorado, (courtesy of Roy Jenne). The global averages are thus based on data from a total of 2201 stations (1545 stations from the NH), each of which has a minimum of 35 years of record in the interval 1921–1960. This reference period was selected because it contained an optimum number of station records. Figure 2 shows the evolution of the temporal coverage for the hemisphere as a whole, as well as

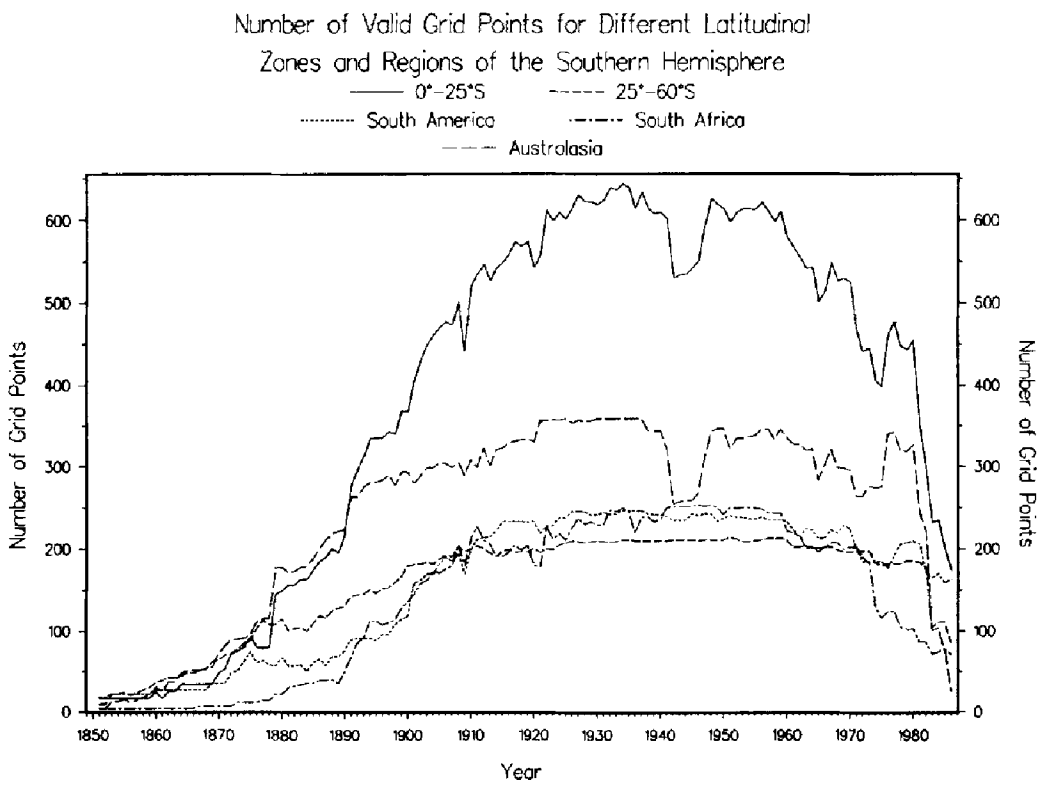

Fig. 2. Graph showing the temporal distribution of grid points for the indicated regions. The first year with at at least 50% or more of the maximum number of available grid points is as follows: 1893 for the 0°–25°S index, 1877 for the 25°–60°S index, 1898 for the South American index, 1894 for the southern African index, and 1879 for Australasia.

for several subregions. The first year containing 50% of the maximum coverage attained is indicated in the figure caption.

Temporal trends were evaluated by simple linear regression, using time as the independent variable, and were calculated over the period from 1890 to 1986 for each precipitation index. Statistical significance against the null hypothesis of zero trend was evaluated by use of the F ratio [*Draper and Smith*, 1981]. Comparisons of selected regional indices, such as the Great Lakes region and the contiguous United States with other precipitation data sets [*National Oceanic and Atmospheric Administation (NOAA)* sets 1983] indicate that both data sets are highly correlated. Similar comparisons of smaller regional indices for the Amazon Basin in South America and the Soviet Union [*Vinnikov et al.*, 1988] suggest that the data give a reasonably good estimate of the large-scale precipitation variability at interannual and decadal time scales. We believe then that with regard to large-scale precipitation averages, biases and errors associated with station homogeneity are minimized to such an extent that meaningful climatic signals can be extracted from the data. Nevertheless, there is still a possibility that indices comprised of a relatively small number of stations (grid points) may not be suitable for analysis of long-term trends prior to testing for station discontinuities and other biases. Also, estimation errors arising from sampling fluctuations may be a problem in some areas, particularly early and late in the record.

3. Results

3.1. *Regional Averages*

The data were first aggregated into three regional groupings (Figure 1): a sector covering South America (0°–60°S, 180°–30°W), another covering southern Africa (0°–60°S, 30°W–60°E), and a third encompassing the southern Australasian region (0°–60°S, 60°–180°E). The longitudinal ranges were arbitrarily chosen, but they encompass the three major continental areas in the southern hemisphere outside of Antarctica. Although the first year with 50% coverage for the individual regions varies from 1879 for Australasia to 1898 for South America, all indices have been plotted starting in 1890 for consistency and ease of comparison.

The resulting time series are shown in Figures 3–5. An increase in mean precipitation is evident principally over the South American sector (Figure 3), although the Australasian area experienced high rainfall amounts during the 1970's (Figure 4). The latter also exhibits strong interannual variability. There is virtually no precipitation trend in the region of southern Africa (Figure 5), in marked contrast to the steep decline evident north of the equator [*Bradley et al.*, 1987*a*]. The positive seasonal and annual trends over the South American region are all statistically significant at the $<5\%$ level, although the largest relative increases occur during the southern winter and spring. Inspection of precipitation time series from the Amazon Basin and from the region south of the Tropic of Capricorn indicates that during Amazonia's wettest season (from December to May), rainfall has been relatively stable for most of this century. However, the drier months of June to November display positive trends, leading to an increase in the annual totals. In the temperate areas, precipitation rose principally during winter (June-July-August; hereafter JJA) and spring (September-October-November; hereafter SON).

A statistically significant increase in southern Africa precipitation occurs only in spring (Figure 5). In the Australasian

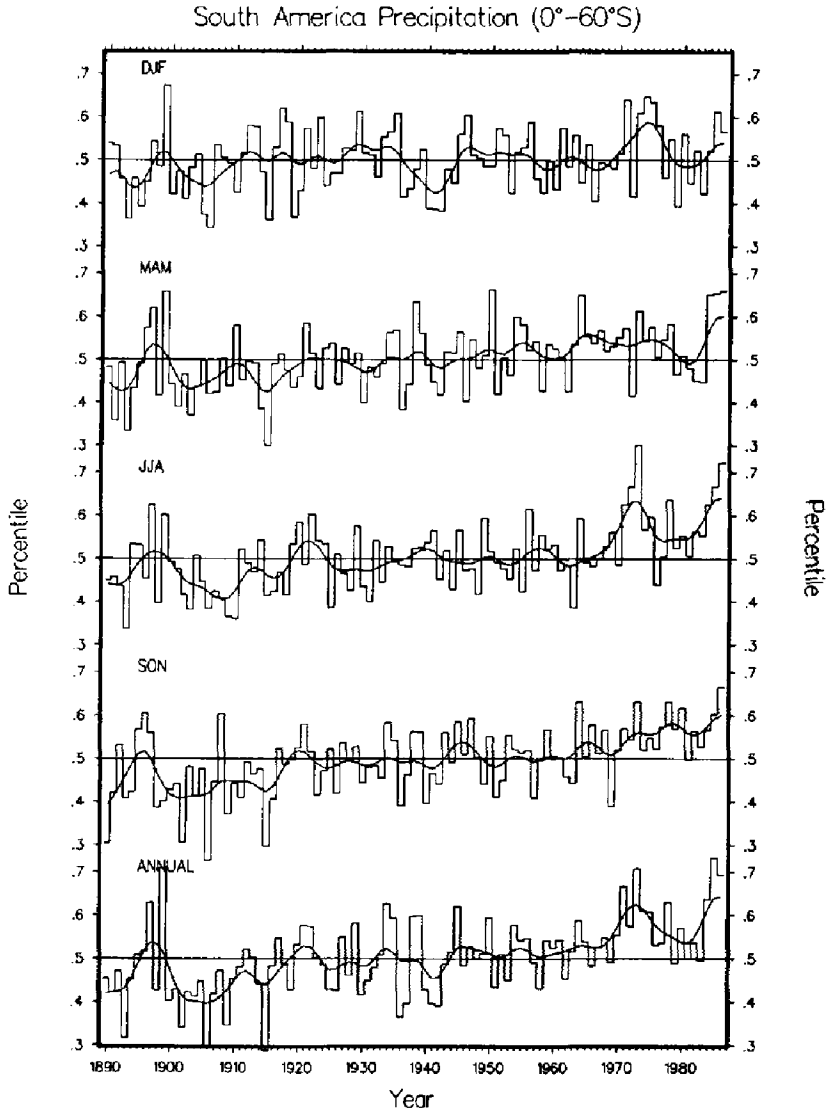

Fig. 3. Seasonal and annual precipitation index (mean of percentiles of the gamma probability distribution at all valid grid points) for the region 0°–60°S, 1800–30°W, for the period 1890–1986. This region is referred to in the text as the South American region.

region, greater rainfall amounts since about 1970 in southern spring, winter, and summer are largely offset by a decrease in winter (JJA) rainfall (Figure 4).

A strong correlation ($r = 0.47$) exists between Australasian and South American precipitation (see Table 1), as illustrated in Figures 3 and 4 and in Figures 6 and 7; this is due at least partly to their strong coupling to the ENSO phenomenon [*Ropelewski and Halpert*, 1987; *Rogers*, 1988; G. N. Kiladis and H. F. Diaz, Global climatic anomalies associated with extremes of the Southern Oscillation, submitted to the *Journal of Climate*, *1988*].

Tropical precipitation indices were also calculated for three meridional sectors from 25°N to 25°S covering the same longitudinal range as in Figure 3–5; they are plotted in Figures 6–8. The increases in rainfall present in South America south of the equator (Figure 3) are not apparent when the region north of the equator is included (Figure 6). Only the September-October period retains a significant positive linear trend, while two of the seasons (December-January-February, hereafter DJF, and March-April-May, hereafter MAM) now have overall negative (though not significant) linear trends. The effects of the 1957–1958 and 1982–1983 ENSO events are clearly evident in the DJF and MAM seasons and the annual mean curve which exhibit record or near-record low values [see *Hastenrath*, 1985; *Rogers*, 1988]. As mentioned earlier, the corresponding precipitation index for the South American sector from 0° to 25°S (not shown) exhibits largest increases in the period from June to November, with only marginal increases occurring during the rainy season from December to May.

The curves covering the Australasian region (Figure 7) show little trend, though the 1970's were quite wet and a decline is evident in recent years. The corresponding rainfall index for the southern Australasian tropics (not shown) indicates opposing seasonal trends, with the solstice seasons (DJF and JJA) showing recent rainfall declines, while the the equinoctial seasons display enhanced rainfall. Annual percentiles rise sharply begining in the late 1960's and have remained relatively high through the early 1980's.

Precipitation trends over tropical Africa differ markedly, depending on whether one is looking at areas to the north or south of the equator. Figure 8 reflects this fact, as the seasons

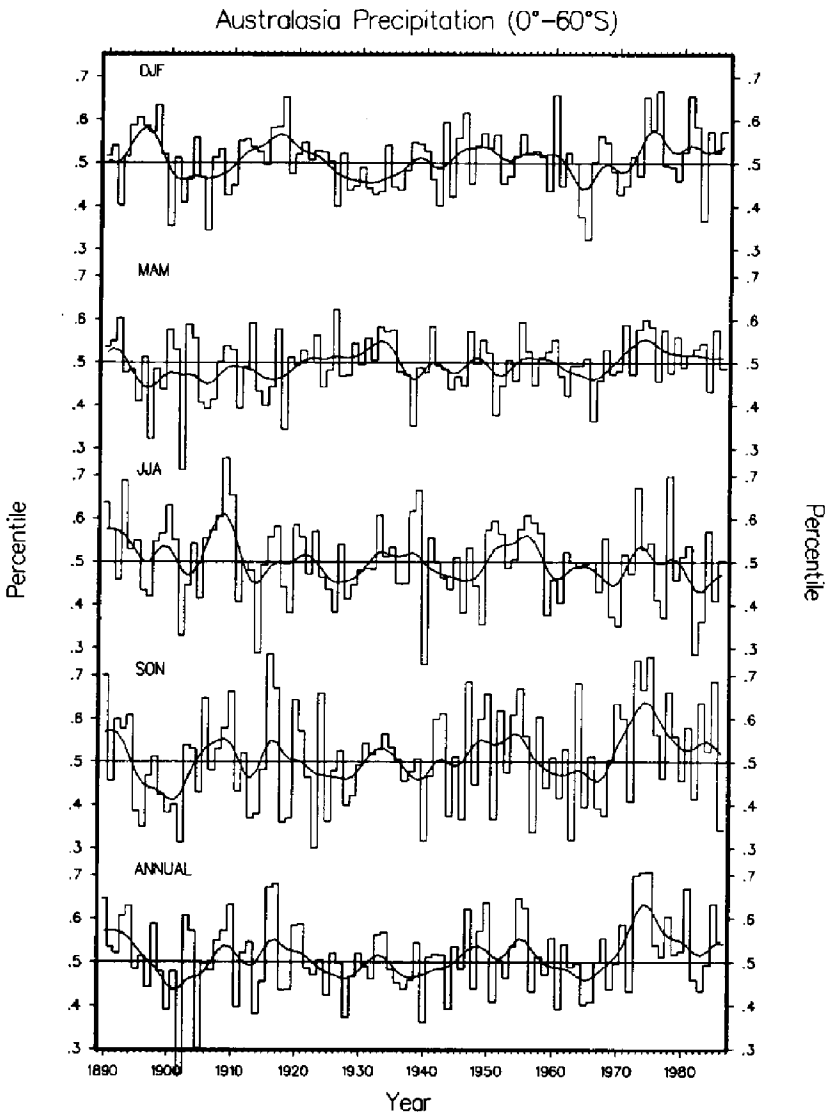

Fig. 4. As in Figure 3, except for the region, 0°–60°S, 60°–180°E, referred to as the Australasian region.

with a significant decrease in rainfall are those associated with the rainy season in tropical northern Africa (JJA and SON), whereas the remaining two seasons, which correspond to the southern rainy season, exhibit little trend. The recent decline in tropical African rainfall is remarkable and represents one of the largest climate signals present in the modern instrumental climate record [see *Lamb*, 1982; *Nicholson*, 1985]. The indices for tropical southern Africa (not shown) are similar to those for the southern Australasian tropics, in that they show a tendency toward lower precipitation during the two solstice seasons and increases during the equinoctial seasons. The annual index, however, exhibits little tendency since the 1950's, although a notable dry period is evident during the 1940's.

In the following section we compare precipitation indices for different zonal belts and develop "hemispheric" and "global" indices from all available data.

3.2. *Zonal, Hemispheric, and Global Indices*

Averages were calculated for two SH zonal bands (0°N–25°S and 25°–60°S). Figure 9 illustrates the variation in precipitation for temperate latitudes (25°–60°S). All five curves exhibit positive linear trends, but only those for the annual spring (SON) and summer (DJF) seasons are significant at the 5% level.

The southern tropics (Figure 10) also display generally positive trends, with the annual spring and autumn seasons containing statistically signficant positive linear trends. The effects of the 1982–1983 warm ENSO episode are clearly indicated, with 1983 summer (DJF) precipitation being the driest such season on record. In general, warm ENSO events are associated with dryness in tropical continental areas [*Bradley et al.*, 1987*b*; *Ropelewski and Halpert*, 1987], whereas in normally dry regions of the central and eastern equatorial Pacific, rainfall increases greatly [*Kiladis and van Loon*, 1988], so that the net zonal mean change may actually be small.

The opposing trends evident over comparable latitudinal bands of the NH are not present here. Furthermore, all curves exhibit greater temporal coherence than their NH counterparts (Table 1). The correlations range from 0.15 for the autumn season (MAM) to 0.45 for the spring season (SON). Except for the autumn season, the correlation coefficients are significant at better than the 5% level.

Indices of annual and seasonal precipitation for the South-

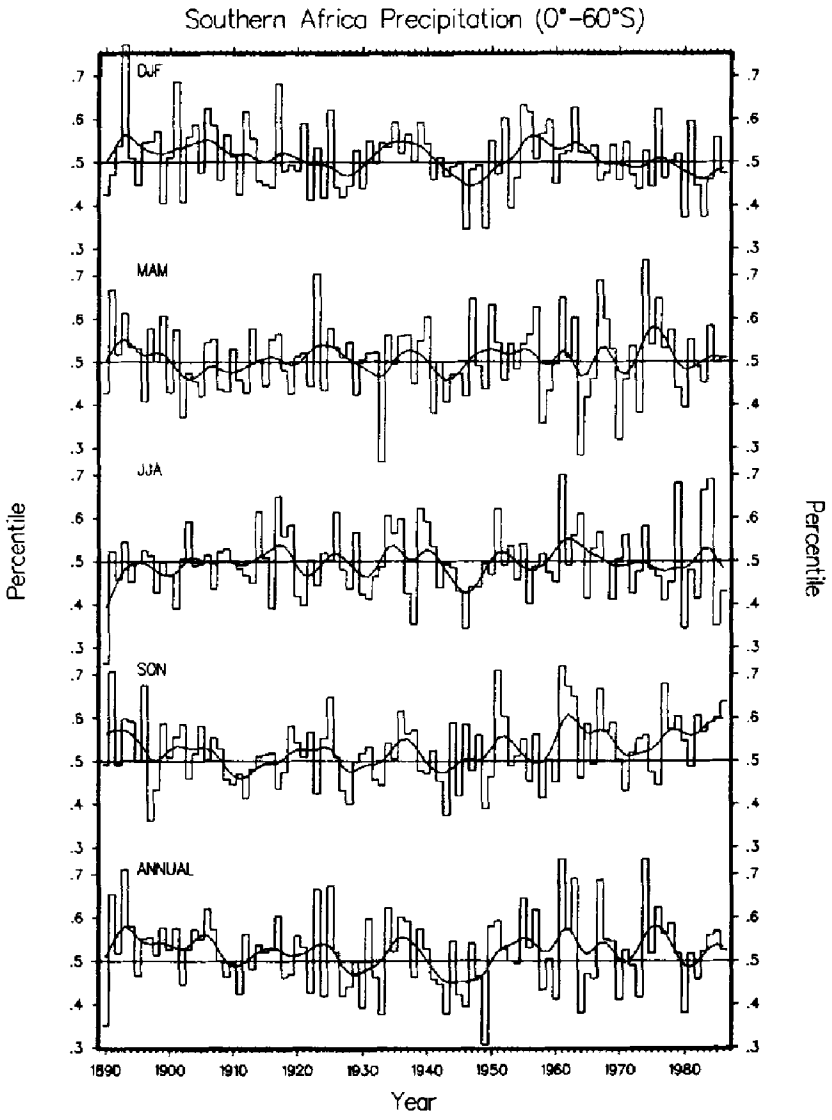

Fig. 5. As in Figure 3, except for the region, 0°–60°S, 30°W–60°E, referred to as the southern Africa region.

ern Hemisphere (0°–60°S) land areas are shown in Figure 11. There appears to have been an overall increase in precipitation beginning in the 1940's. Seasonally, the increase is largest in southern spring, followed by autumn; the trends are smallest in the southern winter and summer seasons, neither of which is statistically significant at the 5% level. Positive linear trends for the period 1890–1986 for the annual MAM and SON seasons are all statistically significant at the 1% level.

TABLE 1. Correlation Coefficients for Selected Precipitation Indices, 1921–1986

Region	Season	Correlation Coefficients (R)
South America versus southern Africa	Annual	0.01
South America versus Australasia	Annual	0.47†
Southern Africa versus Australasia	Annual	0.01
Southern tropical (0°–25°S) versus southern temperate (25°–60°S)	DJF	0.32*
Southern tropical versus southern temperate	MAM	0.15
Southern tropical versus southern temperate	JJA	0.36†
Southern tropical versus southern temperate	SON	0.45†
Southern tropical versus southern temperate	Annual	0.37†
Northern tropics (0°–25°N) versus southern tropics (0°–25°S)	Annual	−0.21
Detrended northern versus southern tropics	Annual	0.19
Northern temperate (25°–65°N) versus southern temperate (25°–60°S)	Annual	0.08
Detrended northern temperate versus southern temperate	Annual	−0.29
Southern hemisphere versus northern hemisphere (0°–60°N and 0°–60°S)	Annual	−0.07
Detrended southern versus northern hemisphere	Annual	−0.19

*Indicates statistical significance at 5% level.
†Indicates statistical significance at 1% level.

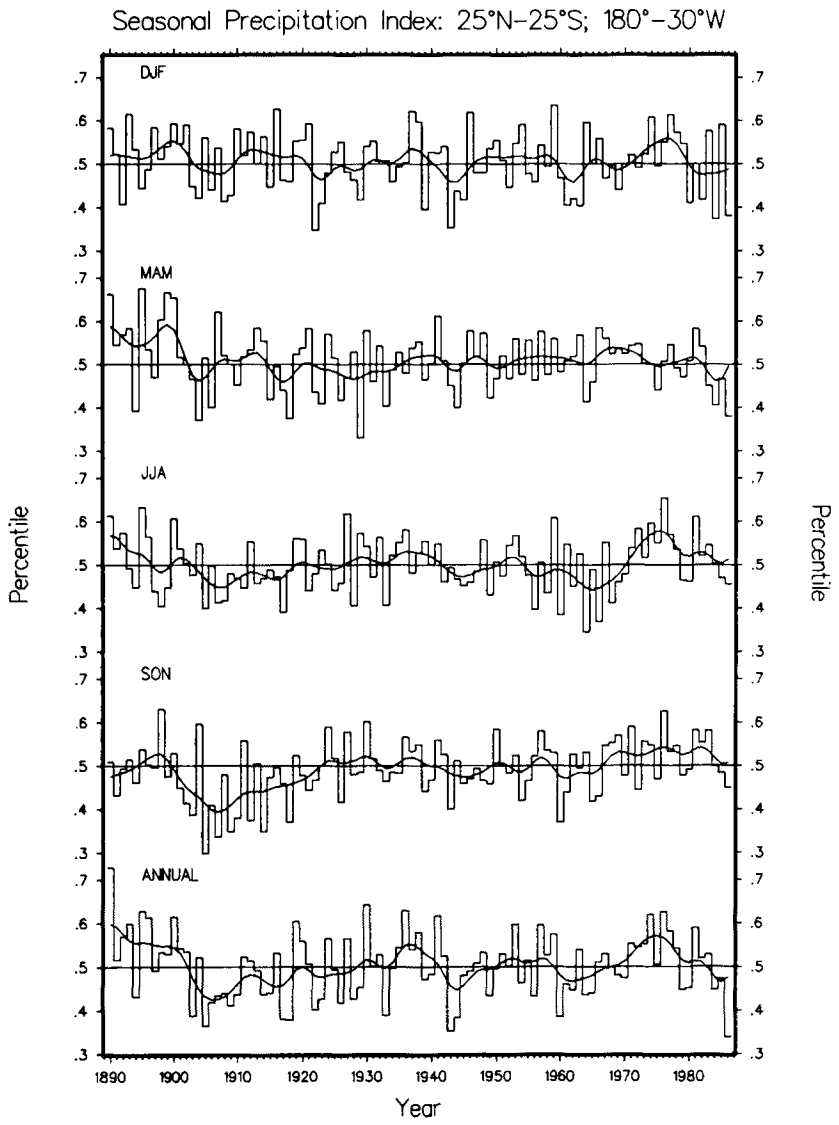

Fig. 6. As in Figure 3, except for the area 25°N–25°S, 180°–30°W, referred to in the text as the South American sector.

The updated and slightly revised NH record is presented in Figure 12. A downward trend is evident in the annual and seasonal curves (except for spring) since the 1950's, with minimum values attained in 1983. The overall trend (since 1890) is only statistically significant for the fall (at the 1% level), mostly because of the presence of low values prior to the 1920's, and for the winter (at the 5% level). The corresponding annual indices for each hemisphere are uncorrelated (see Table 1).

The data were also split into four zonal bands (0°–25°N, 0°–25°S, 25°–60°N, and 25°–60°S) representative of the tropics and temperate latitudes of each hemisphere. Smoothed curves of the corresponding seasonal and annual indices are displayed in Figures 13 and 14, respectively.

A comparison of the precipitation trends in the corresponding tropical and temperate zones of each hemisphere show that while the temperate latitudes exhibit positive trends in both hemispheres (Figure 14), the tropical belts (Figure 13) display a remarkable difference, much of it occurring since the 1960's. As was the case for the NH, the SH temperate record is characterized by the presence of significant variability at the 5- to 10-year time scale. In agreement with the NH, the period from around 1895 to about 1940 was typically dry. The 1920's were generally dry in both the tropics and temperate regions, but the 1930's were generally wetter than normal in the tropics, with dryness prevailing in the temperate zones of both hemispheres. The 1970's and 1980's have been exceptionally wet everywhere, except in the northern tropics. This is due largely to the severe and prolonged drought in the Sahel, but drier conditions have also existed in parts of Central America and the Caribbean as well as the Hawaiian Islands and southeastern Asia, including the Philippines.

The presence of differential trends in the temperature record of different latitudinal zones of the two hemispheres, which has been documented in several recent studies [e.g., *Ellsaesser et al.*, 1986; *Angell*, 1988] is thus valid also with regard to tropical rainfall. This interesting fact bears further study, including investigations using general circulation models.

It is also of interest to note that in a study of secular changes of tropical rainfall regimes, *Kraus* [1955] concluded that "the average annual volume of precipitation decreased rather suddenly at the turn of the century," noting further that

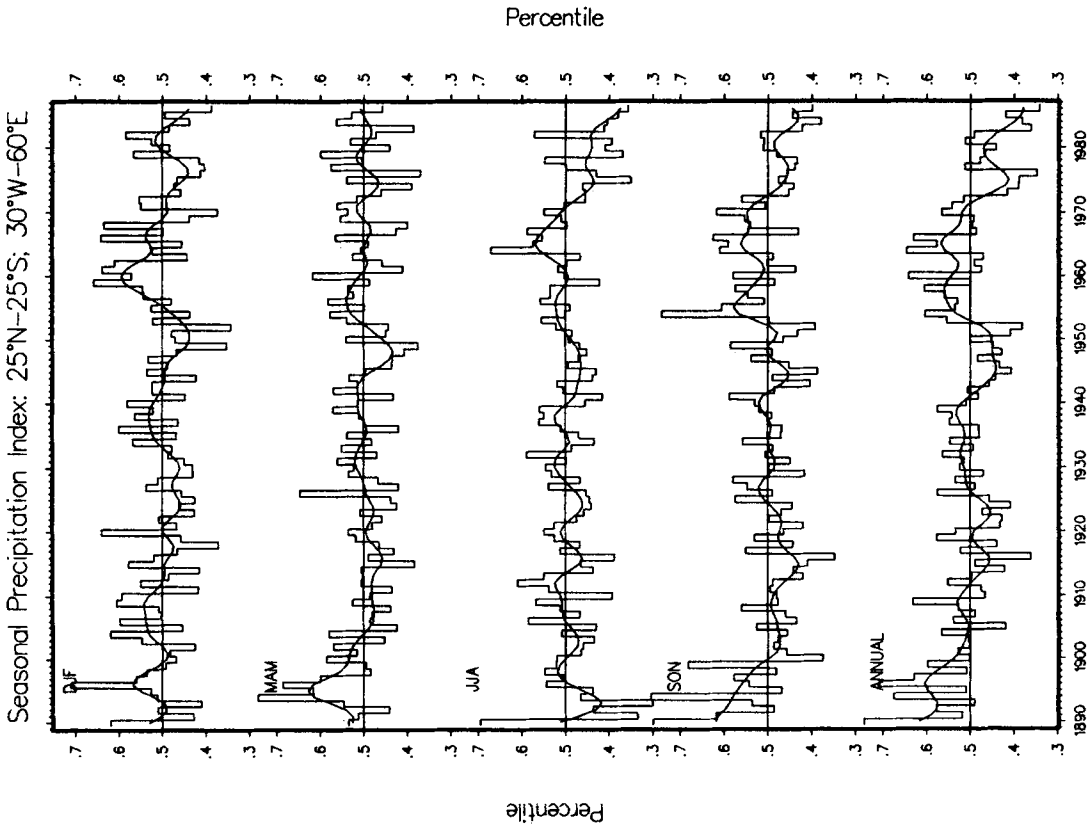

Fig. 8. As in Figure 3, except for the area 25°N–25°S, 30°W–60°E, referred to in the text as the southern Africa sector.

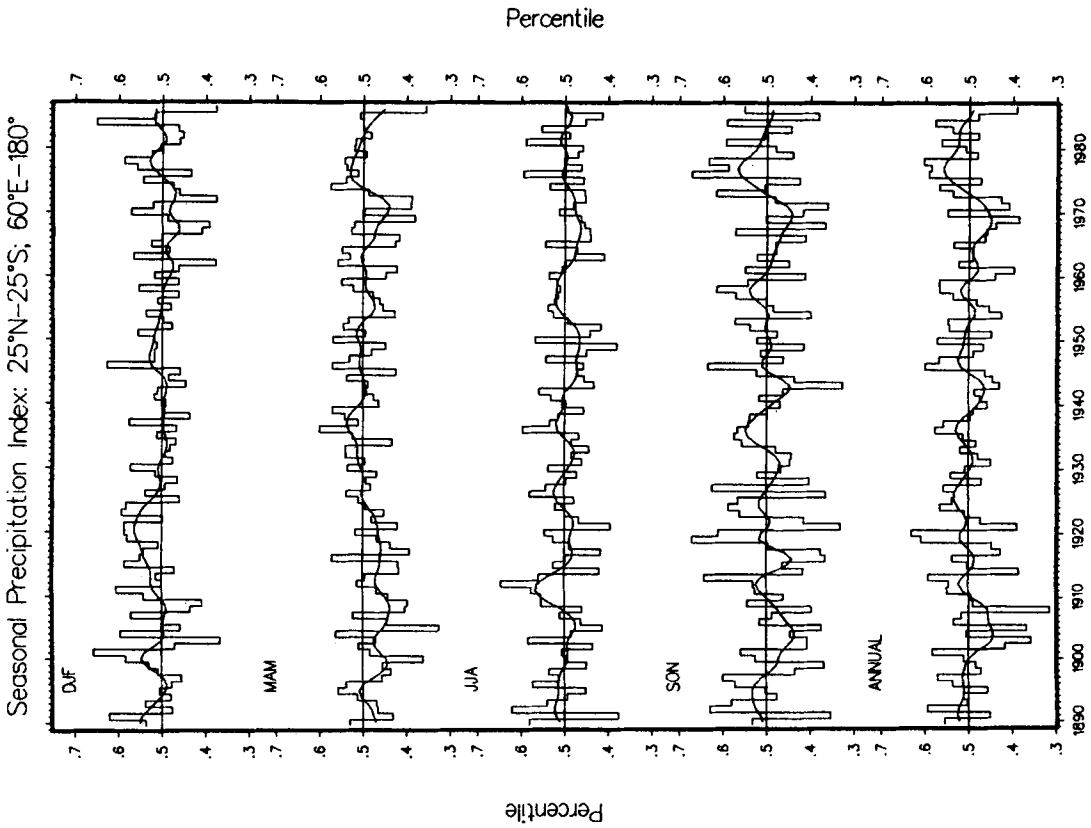

Fig. 7. As in Figure 3, except for the area 25°N–25°S, 60°–180°E, referred to in the text as the Australasian sector.

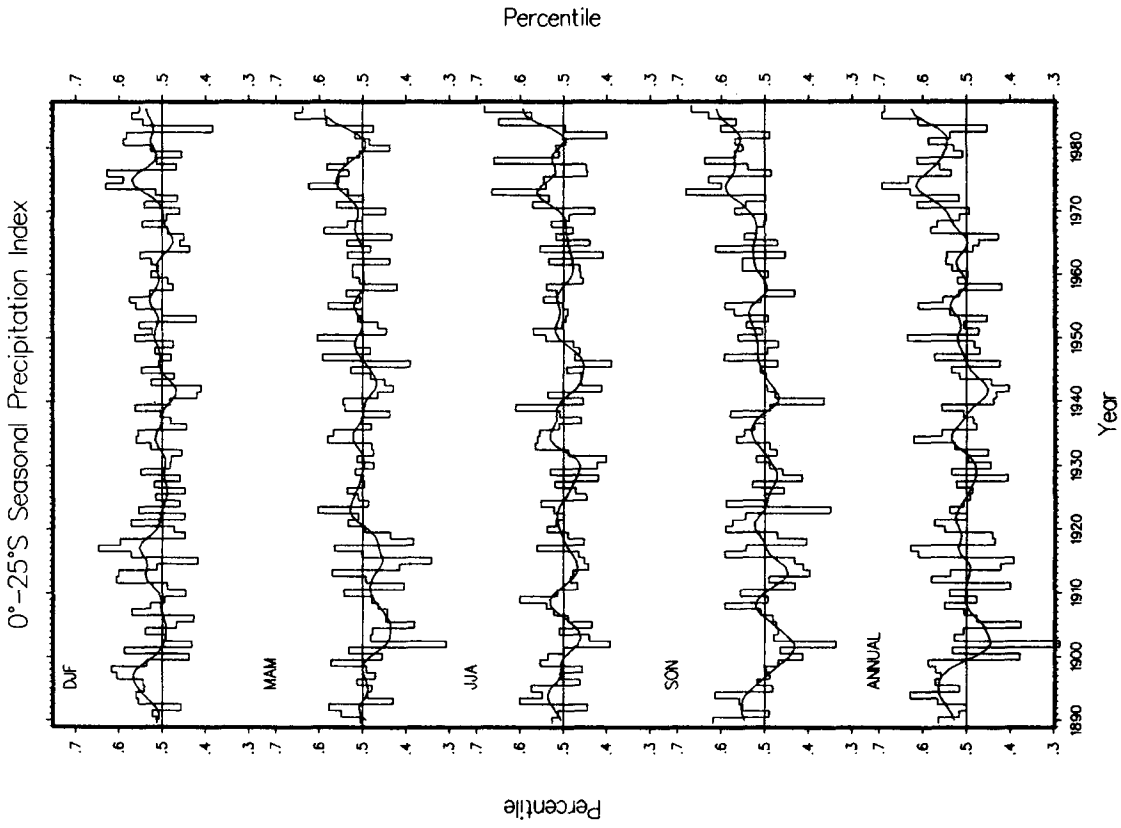

Fig. 10. As in Figure 3, except for the zonal belt 0°–25°S, referred to in the text as the southern tropical region.

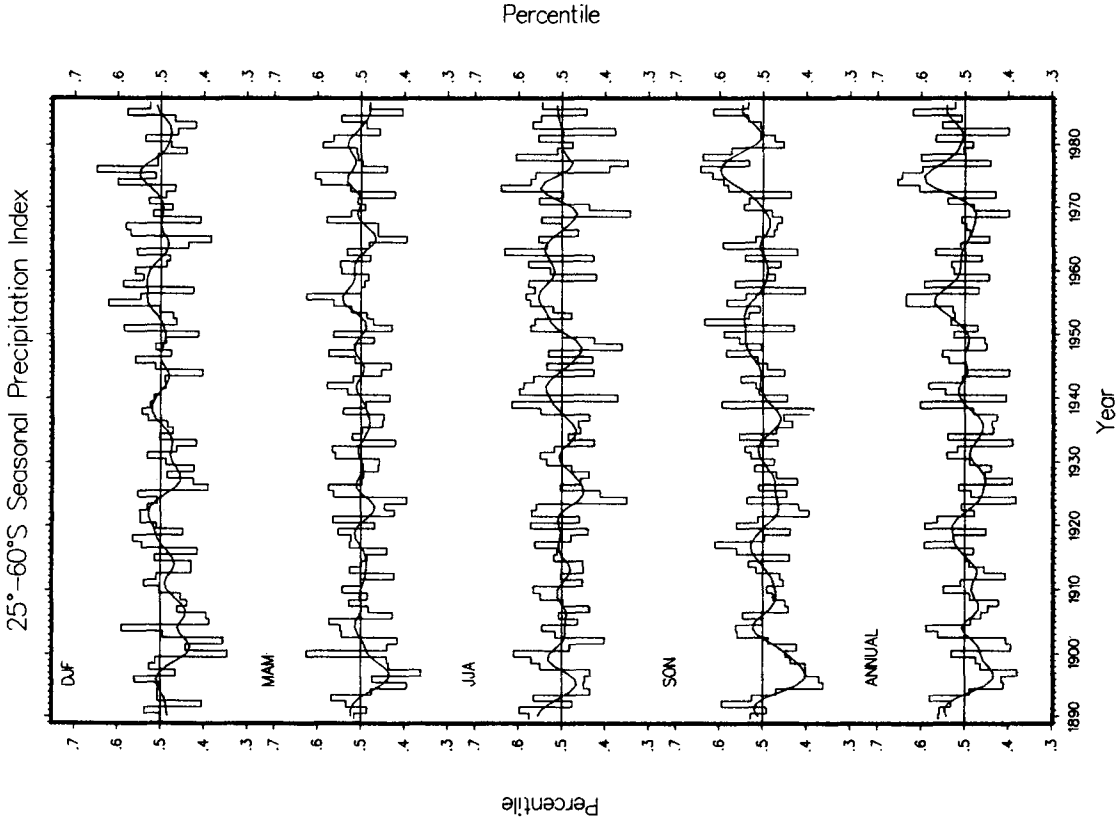

Fig. 9. As in Figure 3, except for the zonal belt 25°–60°S. This is referred to in the text as the southern temperate region.

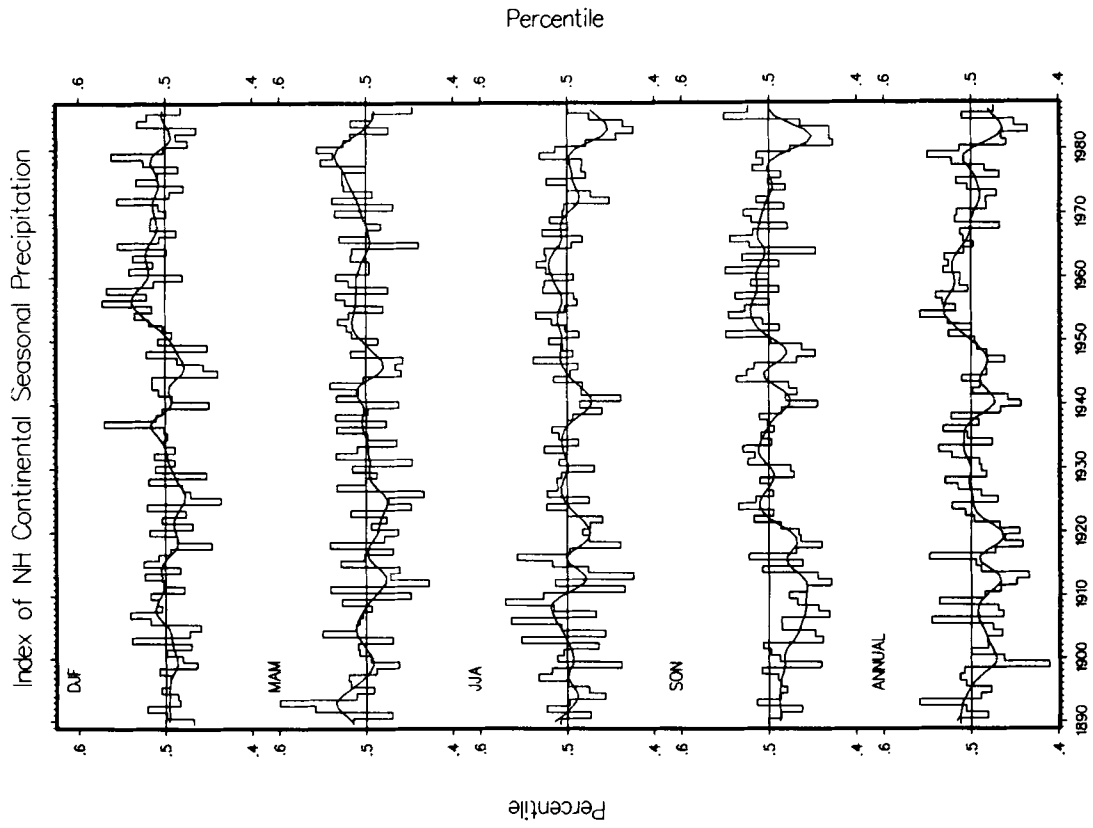

Fig. 12. As in Figure 11, except for the northern hemisphere land areas.

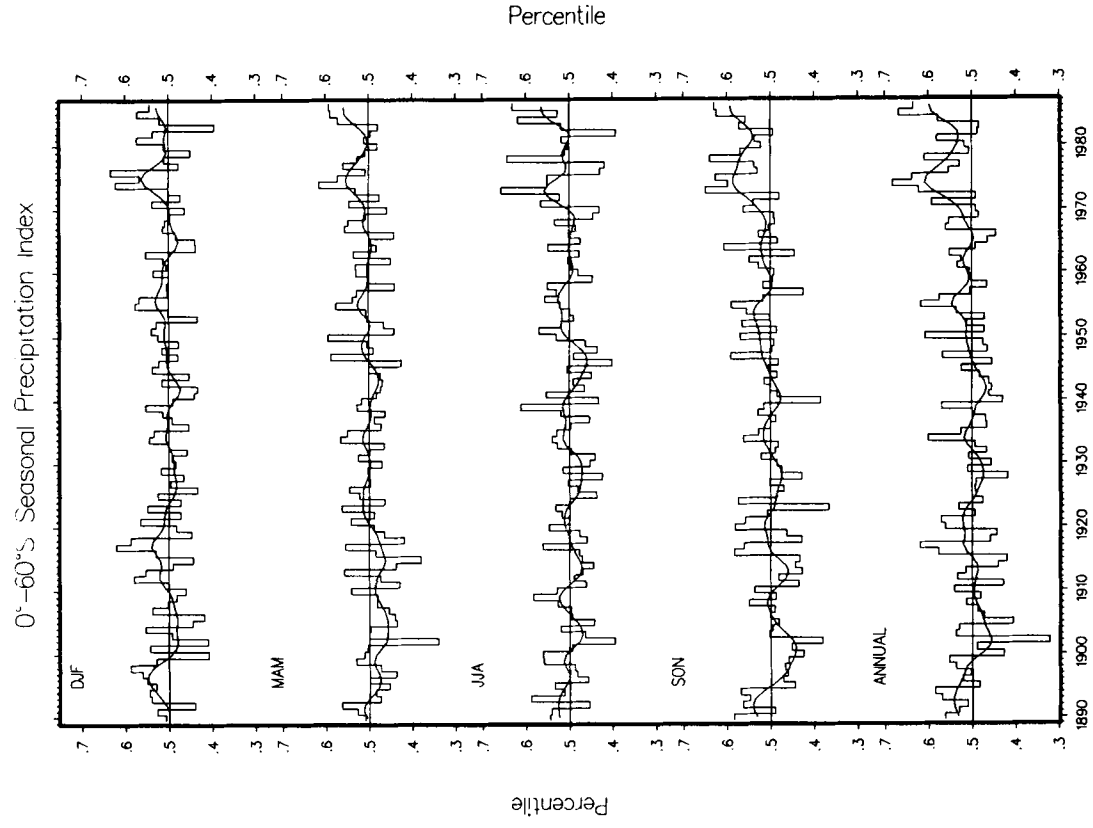

Fig. 11. Seasonal and annual precipitation index (mean of percentiles of the gamma probability distribution at all valid grid points) for the southern hemisphere for the period 1890–1986. The first year in which 50% of the maximum available number of grid points was present is 1890, compared with 1881 for the northern hemisphere.

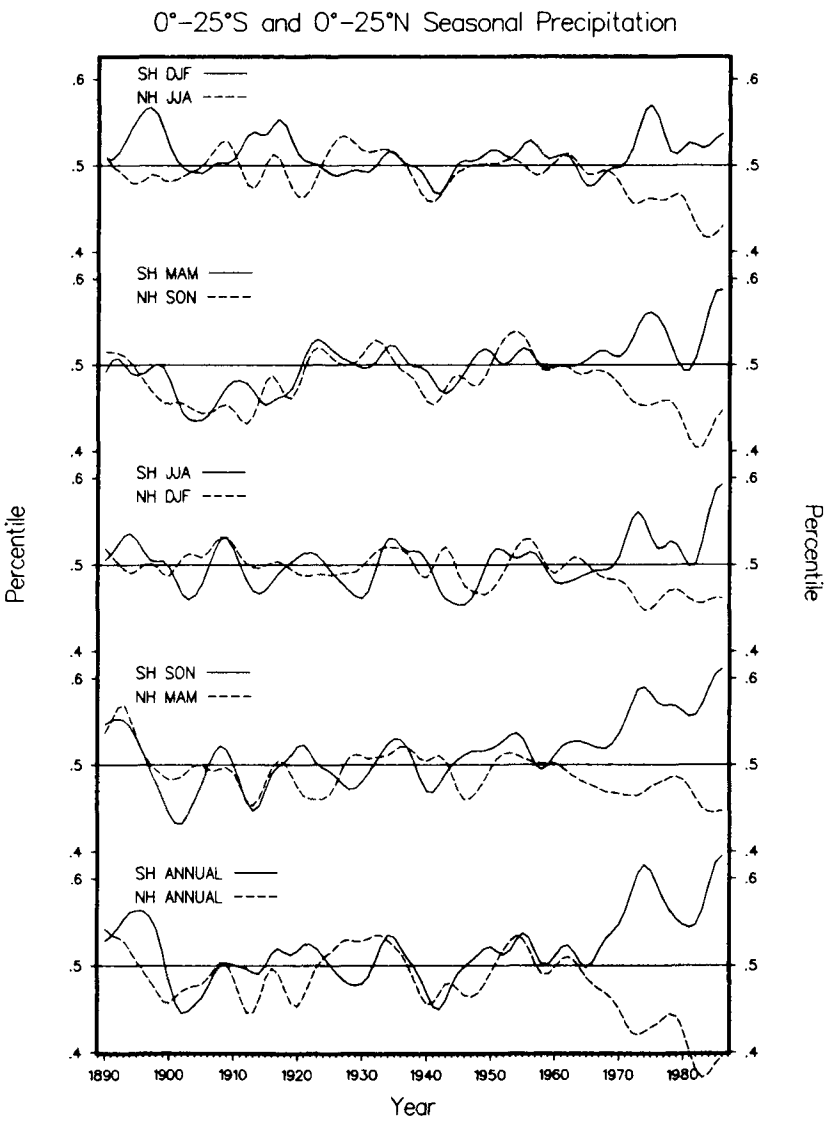

Fig. 13. Time series of the binomially smoothed precipitation indices for the zonal bands 0°–25°N and 0°–25°S.

a change toward drier conditions had also occurred a few years earlier at higher latitudes. Inspection of Figures 9–14 indicates generally good agreement with those results; it further shows that another reversal (toward higher tropical rainfall) took place during the 1940's. With regard to the timing of these changes, there are hemispheric differences. In the NH the shift to greater precipitation at higher latitudes preceded a decrease in the tropics by a decade or so. In the SH, although the decline in precipitation in the 1890's occurred first at high latitudes, the subsequent shift toward higher precipitation occurs at roughly the same time or within a decade of each other.

Kraus [1955] also suggested that the decline in annual mean rainfall "was due largely to a narrowing of the rainfall belt and to a shortening of the wet season." This contention is also supported by our own analysis (not shown) of various tropical subregions, in which we aggregated the data according to the seasonal distribution of the mean annual rainfall. In general, the wet seasons exhibit nonsignificant trends, whereas the drier seasons undergo much greater variation in addition to upward trends in the past decade or two. In many areas the behavior of the rainfall curves follows the temporal pattern noted by Kraus, but with the last 20 or so years displaying a clear tendency toward higher values.

Recently, comparisons have been made of different GCM responses to a doubling of CO_2 by *Schlesinger and Mitchell* [1987], and *Gutowski et al.* [1988]. The equilibrium annual precipitation changes as a function of latitude produced by three different models (the NCAR, Geophysical Fluid Dynamics Laboratory, and Goddard Institute for Space Studies "coupled" models) indicate generally an increase in precipitation at all latitudes (though one model does show drying in northern tropical latitudes). For comparison, we have plotted in Figure 15 the zonally averaged profiles of annual precipitation differences between the recent wet period in middle and high latitudes and the previous 20 years (1976–1986 minus 1956–1975, Figure 15*a*), and the precipitation anomaly for the decade of the 1930's (Figure 15*b*), which is the warmest nominal decade in the northern hemisphere record [*Jones et al.*, 1986*a*]. The zonal profiles for the two periods are substantially opposite in

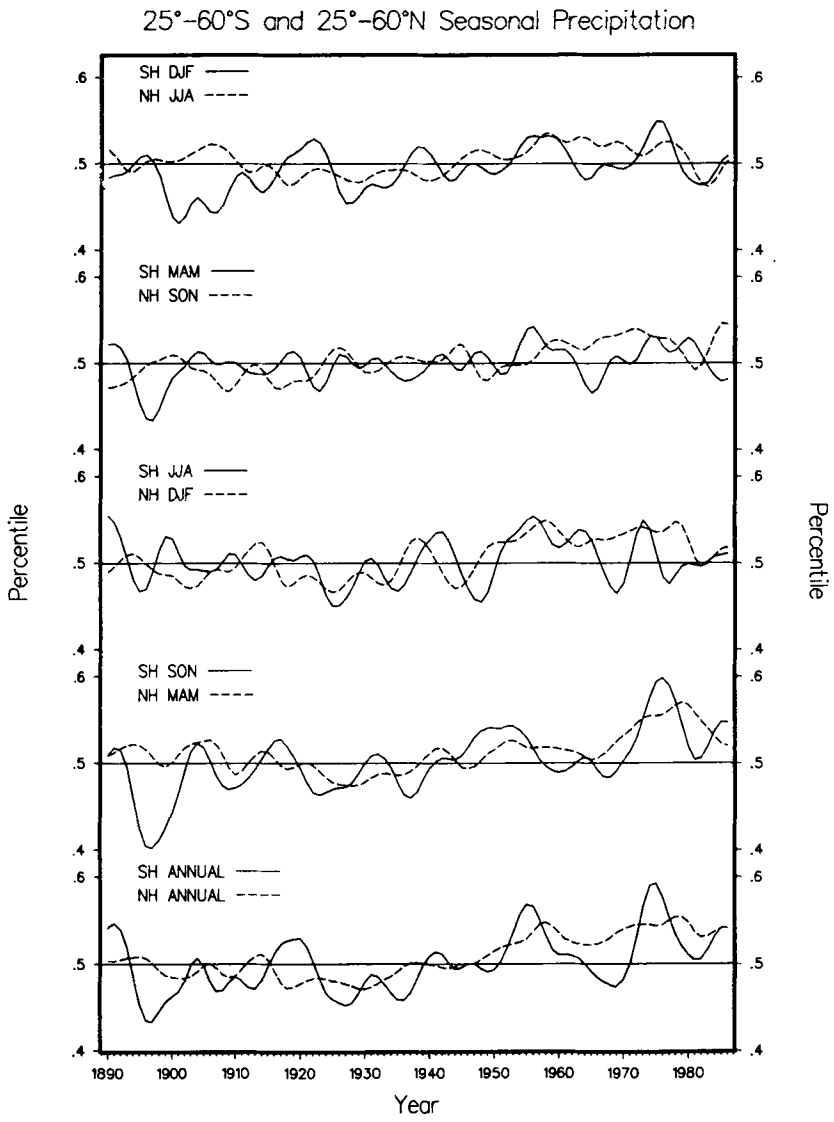

Fig. 14. As in Figure 12, except for the zonal bands 25°–60°S and 25°–60°N.

character, with the recent 12-year period exhibiting mid-latitude wetness and asymmetric tropical responses in the two hemispheres. By contrast, the 1930's show a more coherent interhemispheric pattern with greater tropical rainfall accompanied by mid-latitude drying.

For completeness, we have aggregated the full "global" land domain from 60°N to 60°S, the results are shown in Figure 16. As one might have guessed from the foregoing discussion, the equinoctial seasons exhibit significant upward trends in precipitation, which are reflected in rising annual mean values. The boreal winter season also shows an increase in precipitation during the past 40 years, but the June–August period exhibits little overall trend. Additionally, the years 1982–1984 were quite dry, which is likely a reflection of the extreme ENSO warm event at the time.

4. Possible Causes of Precipitation Changes

Kraus [1955] suggested that the secular changes of tropical precipitation regimes documented in his study were likely related to changes in mean surface wind speed over oceanic regions. Figure 17 illustrates the changes since 1950 in mean scalar wind speed over the oceans averaged betwen the equator and 25°S (see *Woodruff et al.* [1987] for a description of the marine data). A highly significant trend in surface wind speed of about 0.2 m/s per decade is evident. Also shown in Figure 17, for comparison, are the concomitant changes in precipitation over the 0°–25°S tropical band and the temporal changes of sea surface temperature (SST) and surface air temperature for both land and oceans combined. The land data derives from *Jones et al.* [1986*a*, *b*]; the marine data comes from the Comprehensive Ocean-Atmosphere Data Set (COADS). We will discuss the reliability of the observed wind changes later on in this section.

Although *Kraus* [1955] believed the observed changes in SST were of negligible importance in accounting for the relatively large changes in precipitation shown in his study. It is possible that, with regard to the recent increases in SH precipitation shown here, changes in tropical SST have made a substantial contribution. A pronounced increase of about 0.3°C since 1975 in SST and air temperature over both the

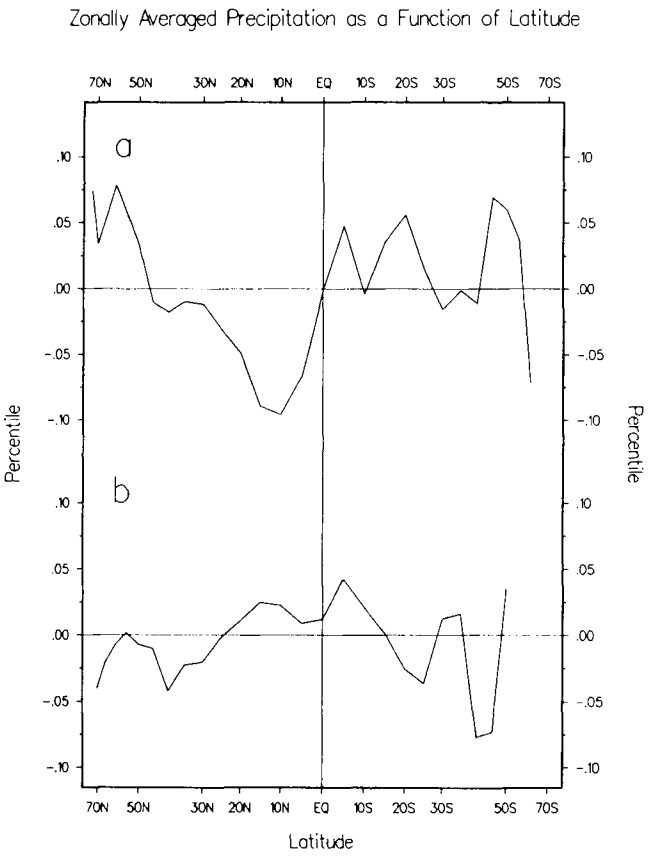

Fig. 15. Zonal-average profiles of precipitation differences for (*a*) the period 1976–1986 minus 1956–1975; and (*b*) the mean deviation for the decade of the 1930's.

land and ocean domains is clearly evident. This should have led to greater evaporation and an increase in moisture content of the lower troposphere over the tropical oceans. The increase in evaporation due to the change in the specific humidities, as derived from the bulk aerodynamic formula for latent heat exchange, is about 10%, which is of the order of the observed changes in precipitation.

It is obvious from Figure 17, however, that there is not a simple one-to-one correspondence between tropical precipitation and tropical SSTs. In fact, while the zonally averaged SSTs and the combined land/ocean surface air temperature data display strong temporal coherence at all time scales ($r = 0.94$), the relationship of both quantities with the annual precipitation curve shown in Figure 16 is actually negative ($r = -0.2$). If you detrend the data, however, the correlation gets larger ($r = -0.6$), which implies a positive association at low frequencies, as is obvious from the graphs. An interesting feature of the plots in Figure 17 is that on the scale of 2–4 years, the influence of ENSO is paramount in modulating tropical climate on a global scale. A relatively large increase in tropical land precipitation is heralded by the end of the 1972 warm ENSO event and the development of cold tropical SSTs in the eastern Pacific from 1974 to 1976.

Recently, several papers have presented evidence of trends in various atmospheric variables over the tropical Pacific Ocean. *Whysall et al.* [1987] concluded that during the period 1950–1981, surface winds in the tropical Pacific had strengthened. *Krahe et al.* (1987) documented a trend toward increasing moisture content at middle tropospheric levels of the tropical Indo-Pacific region. The latter result would be consistent with enhanced evaporation, resulting either from an increase of SST and/or a from strengthening of the surface wind field. More recently, *Hense et al.* [1988] expanded the analysis of *Krahe et al.* to include most of the tropics; their results indicate a general increase of tropical 500- to 700-mbar precipitable water since the mid-1960's, as well as increases in tropospheric mean temperature over the same period. The tropospheric warming would be compatible with enhanced radiative absorption as well as greater latent and sensible heating due to both higher SSTs and an increase in precipitation.

Other studies have documented coherent decadal changes in the surface climatology of the oceans by analyzing several related variables [see *Bunker*, 1980]. There are also indirect measurements which indicate long-term changes in the surface wind climatology. For instance, a study of significant wave-height data over the northeast Atlantic by *Carter and Draper* [1988] indicates a trend toward increasing wave heights over the past 25 years. This would also be consistent with the occurrence of higher wind speeds in that area.

Ramage [1987] and *Wright* [1988], among others, have questioned the reality of the observed wind speed trends, suggesting that they may be largely the result of changes in observational practices. We agree that there are probable inhomogeneities in the ship wind data. However, we do not feel that the full magnitude of the changes can be regarded as simply the consequence of observational biases.

It has been suggested by *Ramage* [1987] that the increase in the proportion of measured (by anemometer) versus Beaufort-estimated winds in the COADS data since 1950 largely accounts for the observed increase in surface wind speeds over the ocean. We have made a comparison of the average wind speed reported by these two methods for two principal ship routes (one in the North Atlantic and the other in the western Pacific). The results show that the average difference in mean wind speed between these two wind reporting methods was only about 0.3 m/s over the 30-year period 1950–1979. Global wind speed comparisons for March and April 1986 (a random selection of months) for both types of wind reporting showed negligible differences. Furthermore, a global map of the linear trend coefficients for the period 1950–1980 indicates that the wind speed changes are spatially variable, being near zero or even negative in some areas and largest in the extratropical North Pacific, where studies have shown a deepening of the Aleutian low-pressure system in recent decades [*Douglas et al.*, 1982; *Diaz and Namias*, 1983]. Even assuming that fully half of the observed trend is spurious, an increase in mean wind speeds over the tropical ocean of around 0.5 m/s over the past 20–30 years results in an increase in evaporation of about 8–9%. Also, a given fractional increase in wind speed will raise the evaporation rate from the ocean surface by at least that much, since an accompanying change in the proportion of higher wind speed categories would also enhance the effective magnitude of the drag coefficient [*Riehl*, 1979].

5. Summary and Conclusions

This paper extends the study of secular precipitation variations for the northern hemisphere land areas performed by *Bradley et al.* [1987*a*], to include the southern hemisphere and other regional averages, including the compilation of a "global" continental precipitation index.

An increase in precipitation from the early 1970's to the

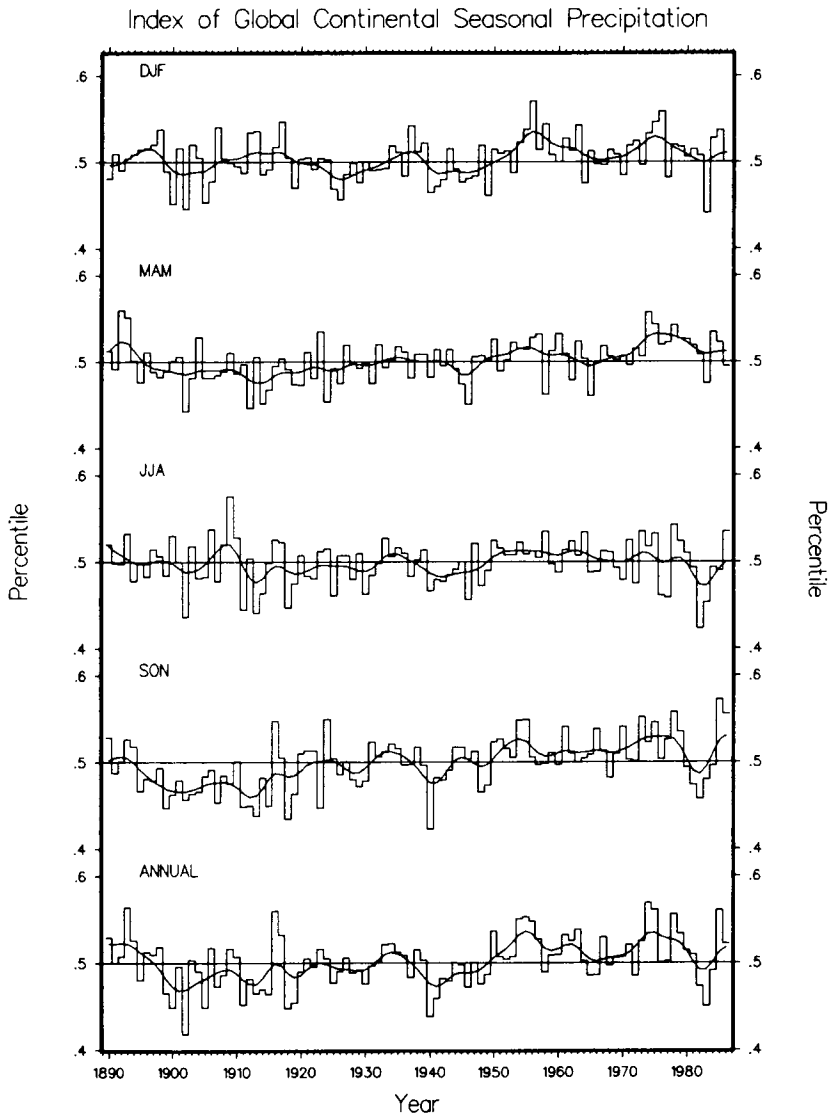

Fig. 16. As in Figure 11, except for the combined land areas of the southern and northern hemispheres (that is, all available grid points) for the period 1890–1984.

mid-1980's was found over temperate southern latitudes, in concordance with similar findings for temperate northern latitudes. On average, tropical southern latitudes also display enhanced rainfall, whereas previous results revealed a significant decrease in northern tropical latitudes. The rise in annual rainfall is due primarily to increases in autumn and spring and then mostly within the South American sector. Interestingly, while there exists a significant negative correlation between annual mean values of the precipitation index for the NH tropical and temperate regions, there is a significant positive association between the corresponding indices in the SH.

This dichotomy is especially strong over Africa, where large declines in annual precipitation have been recorded for northern tropical Africa, but, as shown here, there is little if any trend occurring south of the equator. By contrast, large increases in precipitation are evident throughout South America.

Bradley et al. [1987*a*] noted that the latitudinal distribution of precipitation changes for the NH land areas were not "inconsistent" with the precipitation changes predicted by a suite of general circulation models for doubled CO_2 levels [see *Schlesinger*, 1984; *Schlesinger and Mitchell*, 1987]. The results of this study show latitudinal changes in precipitation over the past several decades that are, in a broad sense, consistent with the same GCM models which generally indicate an increase of precipitation throughout much of the southern hemisphere with a doubling of CO_2 concentrations.

With regard to possible causes of recent precipitation changes, we have pointed out that ship wind observations in the tropics during the past 40 years show an increase in scalar wind speed of the order of 0.4–0.8 m/s. It is entirely possible that this could be largely the result of a slow instrumental or observational bias in the ship winds. However, such an increase would be compatible with increased evaporation from the ocean and observations showing enhanced precipitation in many land areas of the southern hemisphere during the past decade or two. It is also consistent with other studies that show increases in low-level moisture content in the tropical Pacific since about 1960.

The observed increase in tropical SSTs would also result in

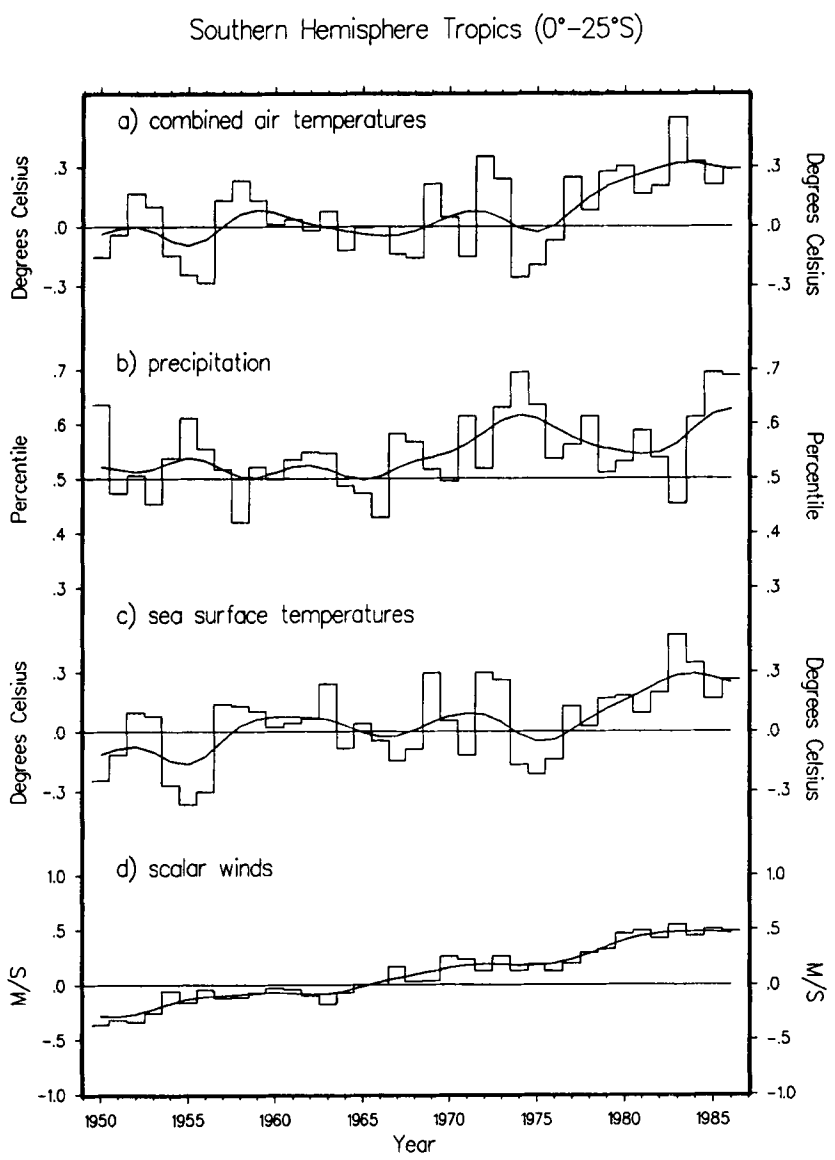

Fig. 17. Trends of zonally averaged anomaly indices for the southern tropics (0°–25°S) for the period 1950–1986: (*a*) combined land and marine air temperature, (*b*) land precipitation index, (*c*) sea surface temperature, and (*d*) scalar mean surface wind. Anomalies for the marine data were calculated from 1950 to 1979 means; for land data anomalies were calculated from 1951 to 1970.

higher evaporation rates and could account, on their own, for most of the precipitation increase. In both instances the assumption is that the increased surface evaporation translates into an actual increase in precipitation (as compared to a change toward higher atmospheric humidities). We should also note that, especially with regard to the southern hemisphere, changes in precipitation over the vastly larger oceanic areas could easily have balanced or even reversed the observed changes over land to yield different zonal averages than those reported here.

Acknowledgments. We thank A. Oort, J. Angell, and the anonymous reviewers for their comments and suggestions on earlier versions of this manuscript. This research has been supported in part by a grant from the Carbon Dioxide Research Division, U.S. Department of Energy (DE-FG02-85ER60316).

REFERENCES

Angell, J. K., Variations and trends in tropospheric and stratospheric global temperatures, 1958–1987, *J. Clim.*, in press, 1988.

Bradley, R. S., H. F. Diaz, J. K. Eischeid, P. D. Jones, P. M. Kelly, and C. M. Goodess, Precipitation fluctuations over northern hemisphere land areas since the mid-19th Century, *Science*, *237*, 171–175, 1987*a*.

Bradley, R. S., H. F. Diaz, G. N. Kiladis, and J. K. Eischeid, ENSO signal in continental temperature and precipitation records, *Nature*, *327*, 497–501, 1987*b*.

Bunker, A. F., Trends of variables and energy fluxes over the Atlantic Ocean from 1948 to 1972, *Mon. Weather Rev.*, *108*, 720–732, 1980.

Carter, D. J. T., and L. Draper, Has the north-east Atlantic become rougher?, *Nature*, *332*, 494, 1988.

Diaz, H. F., and J. Namias, Associations between anomalies of temperature and precipitation in the United States and western northern hemisphere 700 mb height profiles, *J. Clim. Appl. Meteorol.*, *22*, 352–363, 1983.

Douglas, A. V., D. R. Cayan, and J. Namias, Large-scale changes in North Pacific and North American weather patterns in recent decades, *Mon. Weather Rev.*, *110*, 1851–1862, 1982.

Draper, N., and H. Smith, *Applied Regression Analysis*, 2nd ed., 709 pp., Wiley-Interscience, New York, 1981.

Ellsaesser, H. W., M. C. MacCracken, J. J. Walton, and S. L. Grotch, Global climatic trends as revealed by the recorded data, *Rev. Geophys.*, *24*, 745–792, 1986.

Garcia, O., *Atlas of Highly Reflective Clouds for the Global Tropics: 1971–1983*, 365 pp., National Oceanic and Atmospheric Administation, Boulder, Colo., 1985.

Gutowski, W. J., D. S. Gutzler, D. Portman, and W.-C. Wang, Surface energy balance of three general circulation models: Current climate and response to increasing atmospheric CO_2, *Tech. Rep. TR042*, 119 pp., U.S. Dep. of Energy, Washington, D. C., 1988.

Hastenrath, S., *Climate and Circulation of the Tropics*, 455 pp., D. Reidel, Hingham, Mass., 1985.

Hense, A., P. Krahe, and H. Flohn, Recent fluctuations of tropospheric temperature and water vapor content in the tropics, *Meteorol. Atmos. Phys.*, *38*, 215–227, 1988.

Jones, P. D., S. C. B. Raper, R. S. Bradley, H. F. Diaz, P. M. Kelly, and T. M. L. Wigley, Northern hemisphere surface air temperature variations: 1851–1984, *J. Clim. Appl. Meteorol.*, *25*, 161–179, 1986*a*.

Jones, P. D., S. C. B. Raper, and T. M. L. Wigley, Southern hemisphere air temperature variations: 1851–1986, *J. Clim. Appl. Meteorol.*, *25*, 1213–1230, 1986*b*.

Jones, P. D., S. C. B. Raper, C. M. Goodess, B. S. G. Cherry, and T. M. L. Wigley, A grid point surface air temperature data set for the southern hemisphere, *Tech. Rep. TR027*, 73 pp., U.S. Dep. of Energy, Washington, D. C., 1986*c*.

Kiladis, G. N., and H. van Loon, The Southern Oscillation, VII, Meteorological anomalies over the Indian and Pacific Ocean sectors associated with the extremes of the oscillation, *Mon. Weather Rev.*, *116*, 120–136, 1988.

Krahe, P. H., H. Flohn, and A. Hense, Trends in tropospheric temperature and water vapor in the Indo-Pacific region during the last 20 years, *Trop. Ocean Atmos. Newslett.*, *38*, 11–13, 1987.

Kraus, E. B., Secular changes of tropical rainfall regimes, *Q. J. R. Meteorol. Soc.*, *81*, 198–210, 1955.

Lamb, P. J., Persistence of subsaharan drought, *Nature*, *299*, 46–48, 1982.

Maddox, R. A., An objective technique for separating macroscale and mesoscale features in meteorological data, *Mon. Weather Rev.*, *108*, 1108–1121, 1980.

National Oceanic and Atmospheric Administration, State, regional, and national monthly and annual precipitation weighted by area, 68 pp., Nat. Clim. Data Cent., Asheville, N. C., 1983.

Nicholson, S. E., Sub-saharan rainfall 1981–84, *J. Clim. Appl. Meteorol.*, *24*, 1388–1391, 1985.

Ramage, C. S., Secular change in reported surface wind speeds over the ocean, *J. Clim. Appl. Meteorol.*, *26*, 525–528, 1987.

Riehl, H., *Climate and Weather in the Tropics*, 611 pp., Academic, San Diego, 1979.

Rogers, J. C., Precipitation variability over the Caribbean and tropical Americas associated with the Southern Oscillation, *J. Clim.*, *1*, 172–182, 1988.

Ropelewski, C. F., and M. S. Halpert, Global and regional scale precipitation patterns associated with the El Niño/Southern Oscillation, *Mon. Weather Rev.*, *115*, 1606–1626, 1987.

Ropelewski, C. F., and J. B. Jalickee, Estimating the significance of seasonal precipitation amounts using approximations of the inverse gamma function over an extended range, paper presented at Eighth Conference on Probability and Statistics in Atmospheric Sciences, Am. Meteorol. Soc., Boston, Mass., 1984.

Schlesinger, M. E., Climate model simulations of CO_2-induced climate change, *Adv. Geophys.*, *26*, 141–235, 1984.

Schlesinger, M. E., and J. F. B. Mitchell, Climate model simulations of the equilibrium response to increased carbon dioxide, *Rev. Geophys.*, *25*, 760–798, 1987.

Strommen, N. D., and J. E. Horsfield, Monthly precipitation probabilities by climate divisions—23 eastern states, *Misc. Publ. 1160*, 141 pp, U.S. Dep. of Agric. and Commer., Washington, D. C., 1969.

Thom, H. C. S., A note on the gamma distribution, *Mon. Weather Rev.*, *86*, 117–122, 1958.

Vinnikov, K. Ya., P. Ya. Groisman, and K. M. Lugina, The empirical data on modern global climate changes (temperature and precipitation), paper presented at Climate Trends Workshop, Natl. Clim. Prog. Office, NOAA, Washington, D. C., Sept. 7-9, 1988.

Whysall, K. D. B., N. S. Cooper, and G. R. Bigg, Long-term changes in the tropical Pacific surface wind field, *Nature*, *327*, 216–219, 1987.

Woodruff, S. D., R. J. Slutz, R. L. Jenne, and P. M. Steurer, A comprehensive ocean-atmosphere data set, *Bull. Am. Meteorol. Soc.*, *68*, 1239–1250, 1987.

Wright, P. B., On the reality of climatic changes in wind over the Pacific, *Int. J. Climatol.*, *8*, 521–527, 1988.

R. S. Bradley, Department of Geology and Geography, University of Massachusetts, Amherst, MA 01003.

H. F. Diaz, Environmental Research Laboratories, NOAA, 325 Broadway, Boulder, CO 80303.

J. K. Eischeid, Cooperative Institute for Research in Environmental Science, University of Colorado, Boulder, CO 80309.

(Received April 20, 1988;
revised July 22, 1988;
accepted September 23, 1988.)